THZ field generation and manipulation by coherent control over phonon-polaritons

T. Feurer, Joshua C. Vaughan, Nikolay S. Stoyanov, David W. Ward, Keith A. Nelson

Department of Chemistry, MIT, Cambridge, MA 02139

kanelson@mit.edu

Abstract: Here we present experimental demonstrations of coherent control over phonon-polaritons and the associated THz fields by employing spatial-only, temporal-only, and spatiotemporal pulse shaping to steer, focus, and amplify the propagating THz fields. In addition, we show that spatial-only control allows for the generation of specific excitation profiles, including circular excitation geometries that lead to focusing and increased peak amplitude/intensity levels. The polariton host crystals may be uniform or may be patterned into waveguide, resonator, polaritonic bandgap, and other structures. The capabilities enable multiplexed solid-state THz signal generation, signal propagation among specified addresses, signal manipulation, and signal readout, all without loss of bandwidth.

Mixed polar lattice vibrational and electromagnetic modes, called phonon-polaritons, which propagate at light-like speeds through their host crystals are unique and powerful sources of THz radiation. One way to excite them is by non-resonant impulsive stimulated Raman scattering using femtosecond laser pulses. New techniques in spatiotemporal imaging and spatiotemporal and spatial-only femtosecond pulse shaping and structuring of crystal materials have been developed to enable versatile spatiotemporal coherent control over the propagating phonon-polaritons and thereby over the associated THz fields.

Achieving control over propagating coherent responses places new demands on both the excitation and probing processes. In particular, it must be possible to generate excitation light fields that are specified functions of both time and position, and it must also be possible to monitor the time and position-dependent responses. Programmable spatiotemporal femtosecond pulse shaping, through which a single light beam with a single femtosecond pulse may be transformed into many spatially separated light beams, each of which has a specified time-dependent waveform, has been developed [1] and very recently improved [2] to achieve the high fidelity necessary for coherent control applications. Separately, spatiotemporal imaging of propagating, coherent lattice modes has been reported [3]. The combination of these two capabilities enables automated spatiotemporal coherent control over lattice waves that propagate at light-like speeds.

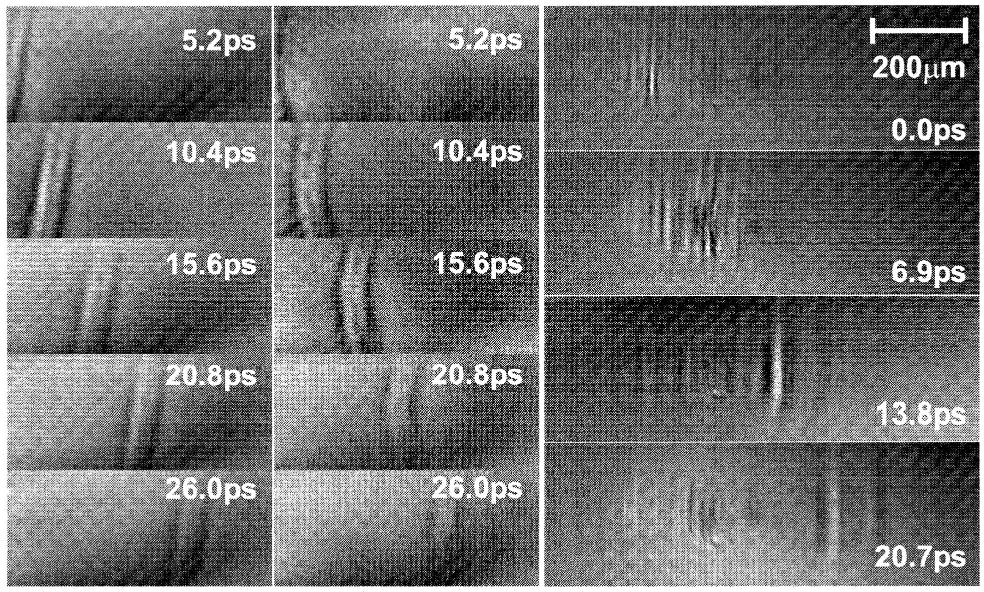

Fig. 1. Polariton responses to a series of about 20 spots, generated through spatiotemporal femtosecond pulse shaping. (LH column) Tilted polariton wavefronts resulting from pulses arriving at excitation spots separated along the vertical dimension at progressively later times, with a linear relation between temporal delay and spatial location of the spot. (center column) Polariton focusing specified through a parabolic relation between temporal delay and spatial location of the spots along the vertical dimension. (RH column) The excitation spots are horizontally arrayed. Excitation pulses arrive at the LH spot first and sweep toward the right, resulting in polariton amplification.

Figure 1 shows results of experiments conducted in $LiTaO_3$ crystals, using 800 nm spatiotemporally shaped excitation waveforms and variably delayed, 400 nm probe pulses. The images of the polariton responses were projected onto a CCD [3]. The LH column shows the result of a linear temporal sweep in which the uppermost excitation spot was irradiated first, then the spot below it, and so on. Different linear sweeps were used to steer polariton responses along selected directions. The center column shows the result of a parabolic temporal sweep in which the first pulses arrived at the top and bottom spots, the next pulses arrived at the adjacent spots, and so on, with the last pulses arriving at the middle spots. Polariton focusing with various focal lengths was conducted by varying the curvature of the parabolic temporal sweep. A combination of linear and parabolic delays was used for both focusing and steering, i.e. to direct focused polaritons to selected locations. The RH column shows polariton amplification, achieved with a sequence of pulses moving from left to right with temporal and spatial delays fixed to match the polariton group velocity. The phonon-polariton response propagating to the right is amplified substantially, while the unamplified responses propagating toward the left are only barely visible.

Besides active coherent control we demonstrate passive control over phonon-polariton propagation by laser-machining integrated waveguide structures on a $LiNbO_3$ platform. Because the wavelengths of phonon-polaritons is typically on the order of a few ten to a few hundred microns, femtosecond laser-machining offers a versatile tool to fabricate waveguides and more complex integrated waveguide structures.

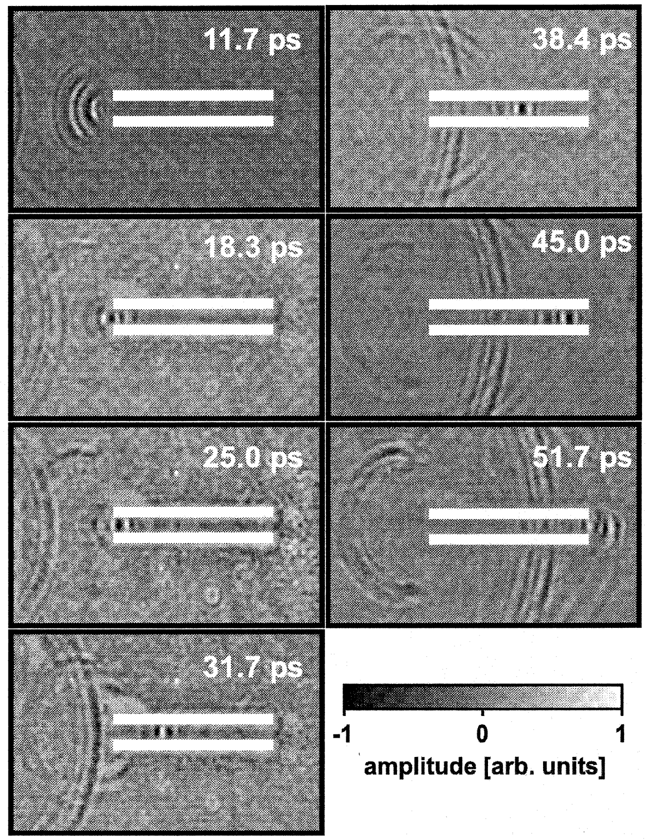

Fig. 2. Phonon-polariton propagation in a laser-machined waveguide structure.

Figure 2 shows a series of snapshots of a phonon-polariton being focused into a laser-machined waveguide structure. The waveguide is 0.2 mm wide and 1.7 mm long. The walls of the waveguide appear blurry, because the CCD camera was moved out of the image plane to achieve high contrast phase imaging. The white bars have been added by image processing and indicate the location and width of the waveguide walls. Immediately after entering the waveguide the phonon-polariton wavefront becomes perfectly plane and remains so until the phonon-polariton exits the waveguide. The last image shows the diverging phonon-polariton as it comes out of the waveguide.

More complex structures, for example an integrated Mach-Zehnder interferometer, have been fabricated and their functionality has been shown.

Applications of our results include programmable generation of user-defined THz waveforms, nonlinear THz frequency spectroscopy, and THz-bandwidth signal processing applications.

Acknowledgement

This work was supported in part by National Science Foundation grant no. CHE97-13388 and MRSEC program award no. DMR98-08941, and Army Research Office grant no. DAAD19-99-1-0034. T. Feurer acknowledges financial support by the Max Kade Foundation.

References

1. R.M. Koehl, T. Hattori, K.A. Nelson, Opt. Commun. **157**, 57 (1998)
2. T. Feurer, J.C. Vaughan, R.M. Koehl, K.A. Nelson, Opt. Lett. **27**, 652 (2002)
3. R.M. Koehl, S. Adachi, K.A. Nelson, J. Phys. Chem. A **103**, 10260 (1999)